# Neutron resonance parameters and thermal-neutron capture by $^{43}$Ca

M. C. Moxon,* J. A. Harvey, and S. Raman
*Oak Ridge National Laboratory, Oak Ridge, Tennessee 37831*

J. E. Lynn
*Los Alamos National Laboratory, Los Alamos, New Mexico 87545*

W. Ratynski
*Soltan Institute of Nuclear Physics, Otwock-Swierk, Poland*
(Received 3 February 1993)

Neutron transmission measurements have been carried out on a small sample (205.9 mg) of $CaCO_3$ with a $^{43}$Ca enrichment of 49.1%. The parameters (spins and neutron widths) of eight resonances below the neutron energy of 20 keV have been determined. This information was combined with a previously measured thermal-neutron coherent scattering length to deduce the separate scattering lengths for the two spin states present in $s$-wave scattering. These values were used to calculate the direct (potential + valence) capture cross sections of the primary electric-dipole gamma transitions in $^{44}$Ca using optical-model potentials with physically realistic parameters. For those states below 6.2 MeV for which the $l=1$ $(d,p)$ spectroscopic factors are known, the experimental cross sections are consistent with our current understanding of the direct and compound-nuclear capture processes. The processes leading to states above 6.2 MeV require further experimental and theoretical studies.

PACS number(s): 25.40.$-$h, 25.40.Dn, 25.40.Lw, 27.40.+z

## I. INTRODUCTION

Of the six stable isotopes of calcium, five are even ($^{40}$Ca, $^{42}$Ca, $^{44}$Ca, $^{46}$Ca, and $^{48}$Ca) and one is odd ($^{43}$Ca). The total thermal-neutron capture cross sections of the even ones are small, ranging from 0.2 to 1.1 b [1], typical of truly off-resonance behavior. In previous papers [2–4] we have analyzed the available data on the primary $E1$ transitions in thermal-neutron capture by the even calcium isotopes and have established that the direct mechanism [5,6] involving the fall of a single-particle $s$-wave neutron to the $p_{3/2}$ or $p_{1/2}$ single-particle final state plays a major role. In all cases except capture by $^{44}$Ca, the agreement between theory and data was quite good, and in the case of $^{44}$Ca, the relatively poor agreement could be explained by considering the modifications to the theory resulting from the collective vibrations of the core. It is plausible that in most of these cases there is some contribution from compound-nuclear effects, but the fact that these contributions are small is certainly consistent with the excited levels of the compound system being widely spaced. Furthermore, there is no evidence that for any of these nuclides a bound or an unbound level lies close to the excitation energy brought in by the thermal neutron.

In previous papers [2,3] $^{43}$Ca was omitted because the thermal-neutron capture process in this odd isotope is qualitatively different from that in the even isotopes. The excitation energy is much higher (the neutron separation energy of $^{44}$Ca is 11.13 MeV rather than in the range 5.14–8.36 MeV across the even isotope sequence), and this high value leads to a much smaller level spacing (of the order of 5 keV per spin state rather than tens or hundreds of keV), thus resulting in much stronger compound-nuclear effects. The thermal-neutron capture cross section (6.2 b) of $^{43}$Ca [1] is much higher than those for the even isotopes, thus indicating the appreciable influence of one or more compound-nuclear levels.

The most significant contributor to the thermal-neutron cross section in $^{43}$Ca is almost certainly the strong resonance at 1.5 keV neutron energy. It has been calculated [7] that the contribution from valence capture to the total radiation width of this resonance is small. Yet the high-energy half of the primary capture gamma-ray spectrum in $^{44}$Ca at thermal neutron energy [8] is correlated with the $p$-wave spectroscopic factors [from the $(d,p)$ reaction [9]] of the final states, and this correlation is normally taken as evidence of direct (potential + valence) capture. Because the interplay between direct and compound-nuclear mechanisms of capture appears to be more evenly balanced in $^{43}$Ca than in many other light nuclides, it is of interest to analyze this case in some detail.

As discussed in earlier papers [5,6] a very important parameter controlling the magnitude of the direct-capture cross section is the neutron coherent scattering length $a$. This quantity was unknown for $^{43}$Ca until recently. It has now been measured via neutron-diffraction measurements [3] at Oak Ridge (Research Reactor) and Argonne (Intense Pulse Neutron Source) as part of a comprehensive study of all stable Ca isotopes. The mea-

*Visitor from AEA Technology, Harwell Laboratory, Oxfordshire, United Kingdom.

 

sured value for thermal neutrons is $a = -1.50 \pm 0.09$ fm.

In Ref. [10] we carried out a preliminary analysis of the capture data [8], but this analysis was not definitive enough because we lacked knowledge of other key parameters required for the calculation, namely, the separate thermal-neutron scattering lengths for the capturing $3^+$ and $4^+$ states as well as the resonance parameters for the 1.5 keV resonance. To remedy this situation, a high-resolution total cross-section measurement on a small sample of $^{43}$Ca has been carried out at the Oak Ridge Electron Linear Accelerator (ORELA) from about a few eV to 500 keV. With this measurement, we have established the spins and neutron widths of the eight most significant resonances below 20 keV. From these parameters, we can infer a quite good estimate of the thermal-neutron scattering length for one of the two possible spins (that associated with the 1.5 keV resonance) and, when combined with the thermal-neutron coherent scattering length measured earlier [3], that for the other spin. Even better information can be obtained if the asymmetry of the cross section (caused by potential-scattering–resonance interference) in the wings of the 1.5 keV resonance can be measured. The thickness of the current sample is insufficient for this purpose, but we have been able to make effective use of some unpublished data obtained at ORELA over 20 years ago with a thicker and more enriched $^{43}$Ca sample.

The new measurements are described briefly in Sec. II, and the analysis leading first to the resonance parameters and then to the scattering lengths are discussed in Sec. III. These scattering lengths, in turn, allow the calculation of the direct-capture cross sections for the primary electric-dipole ($E1$) transitions to final states of $^{44}$Ca with known spectroscopic factors and known or assumed spins. These calculations and comparisons with spectral data are given in Sec. IV. The relative roles of direct, valence, and compound-nuclear capture processes are discussed in Sec. V. Finally, a summary is provided in Sec. VI.

## II. MEASUREMENTS

The neutron transmission measurements from 5 eV to 500 keV were made at a station located 79.34 m from the ORELA water-modulated tantalum target. The sample was 205.9 mg of $CaCO_3$ ($^{43}$Ca enrichment 49.1%) contained in a 0.621-cm-diam graphite holder. The sample thickness $N = 19.57 \times 10^{-4}$ molecule $b^{-1}$ of $CaCO_3$ (or only $9.01 \times 10^{-4}$ atom $b^{-1}$ of $^{43}$Ca) is near optimum for determining the parameters of the 1.5-keV resonance. The neutron detector was a $^6$Li glass scintillator, 12.5 mm thick $\times$ 11.1 cm diam, mounted in a 0.025-mm-thick $\times$ 15-cm-diam Mylar reflecting cylinder between two RCA 8854 photomultiplier (PM) tubes. The PM bases are gated off for 8 $\mu$s to minimize the effects of the gamma flash. To minimize background further, a coincidence is made between the two PM tubes and the resulting signal is used to gate the integrated sum from both PM tubes. The accelerator was operated with burst widths of 19 ns, a repetition rate of 400 pulses per second, and 15 kW of electron beam power. A 0.30 g cm$^{-2}$ $^{10}$B filter was used to reduce overlap neutrons and a 0.64-cm-thick lead filter to reduce the effects of the gamma flash (gamma rays from the capture of thermal neutrons in the tantalum target and the water moderator).

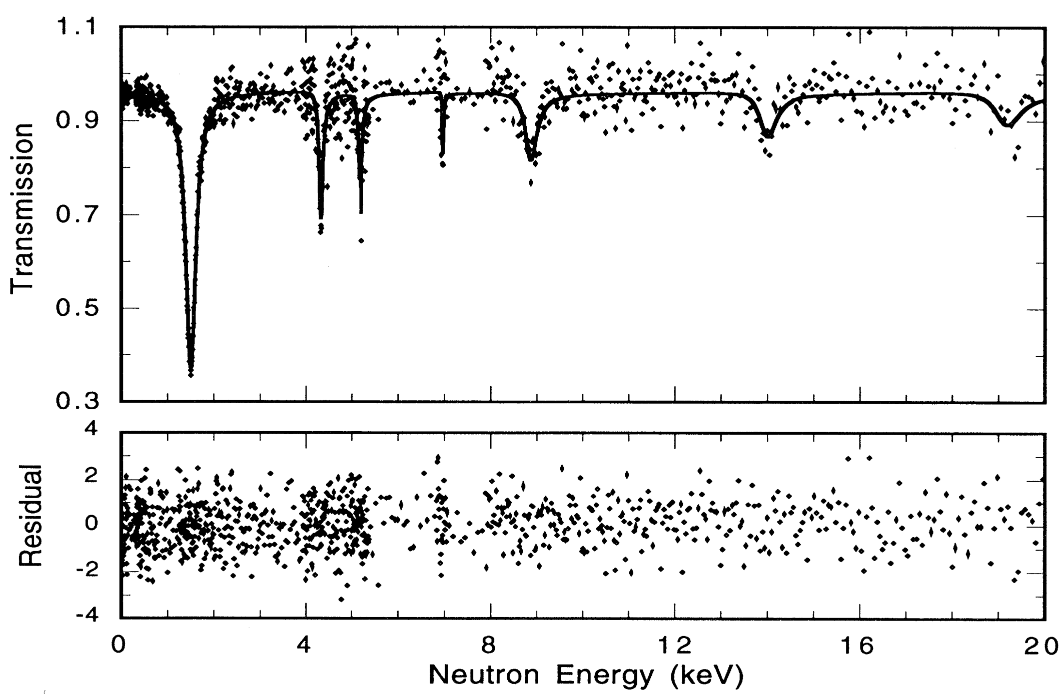


FIG. 1. Neutron transmission data obtained at a flight path of 79.34 m with an enriched $CaCO_3$ target ($9.01 \times 10^{-4}$ atom $b^{-1}$ of $^{43}$Ca). Also shown are calculated curves based on the deduced resonance parameters given in Table I. The residuals (measured − calculated) are in units of one standard deviation.

The time-of-flight data were corrected for the dead time (1104 ns) of the time digitizer and for the backgrounds, which, in general, totaled less than 3% of the observed count rate over the measured energy range. These backgrounds consist of a constant beam-independent background, a $T_{1/2}=17.6$ $\mu$s gamma-ray background from the capture of the neutrons in the water moderator, and a time-dependent background arising from neutrons scattered from the $^{6}$Li glass detector. The resultant transmission is shown in Fig. 1.

## III. DATA ANALYSIS

The total cross sections have been analyzed using the computer program REFIT [11], which carries out a least-squares fit to the transmission data to determine the nuclear parameters used in the theoretical $\mathcal{R}$-matrix expression for the cross section

$$\sigma_{n,\text{tot}}=(2\pi/k^2)\sum_J g_J(1-\text{Re}U_J) , \tag{1}$$

where $k$ is the neutron wave number for neutrons of energy $E$ and $g_J$ is the spin-weighting factor $(2J+1)/2(2I+1)$ for a target nucleus of spin $I$. If no other reaction channel is open, the collision function for $s$-wave neutrons is

$$U_J=\exp(-2ika_c)[(1-ika_c\mathcal{R}_J)/(1+ika_c\mathcal{R}_J)] , \tag{2}$$

where

$$\mathcal{R}_J=\sum_{\lambda(J)}\gamma^2_{\lambda(n)}/(E_\lambda-E) \tag{3}$$

and the sum runs over resonance levels $\lambda$ with spin $J$, neutron energy $E_\lambda$, and reduced neutron width $\gamma^2_{\lambda(n)}$. The quantity $a_c$ is the channel radius in the neutron channel; for $s$-wave neutrons it can be assigned a value close to the nuclear potential radius $R$.

The $\mathcal{R}$ function can be split into two terms, one a local term $\mathcal{R}_J^{\text{loc}}$ containing explicit reference only to local levels (with neutron widths $\Gamma_{\lambda(n)}$) close to the energy range under analysis, and a term $\mathcal{R}_J^{\infty}$ containing the essentially energy-independent contribution of more distant levels, including the very long-range optical-model effects. Thus

$$\mathcal{R}_J=\mathcal{R}_J^{\text{loc}}+\mathcal{R}_J^{\infty}=\sum_{\lambda(\text{loc})}\frac{\Gamma_{\lambda(n)}/2kR}{E_\lambda-E}+\mathcal{R}_J^{\infty} . \tag{4}$$

The cross section is Doppler-broadened numerically in REFIT, but for most of the broad $s$-wave resonances found in the cross section of $^{43}$Ca, the Doppler effect is small. The neutron transmission given by

$$T=\exp(-N\sigma_{n,\text{tot}}) , \tag{5}$$

is convoluted with the experimental resolution function, and it is this $T_{\text{eff}}$ that is finally compared with experiment. The program REFIT is able not only to handle sophisticated and realistic forms of the resolution function but also to readjust normalization constants and backgrounds iteratively until optimum fits are obtained. The sample used in the current measurements is so thin that the analysis was found to be very insensitive to the value of $\mathcal{R}_J^{\infty}$, which, in the final analysis, was assumed to be zero. The spin $I$ of the target nucleus $^{43}$Ca is $\frac{7}{2}$, thus allowing $s$-wave resonances to have possible spins 3 and 4. Because the radiative capture width ($\sim 0.6$ eV) is negligible compared to the neutron width ($\sim 200$ eV) for nearly all the analyzed $s$-wave resonances, the spins are determined unambiguously from the observed peak cross sections (minimum transmissions) of the resonances. The neutron widths (and, hence, the reduced neutron widths $\gamma^2_{\lambda(n)}=\Gamma_{\lambda(n)}/2ka_c$) are also reasonably well determined by analyzing the data from this particular sample. The nuclear parameters determined in this analysis are presented in Table I.

Transmission measurements made earlier at ORELA on thicker samples ($N=17.18\times10^{-4}$ atom b$^{-1}$ and $N=251.8\times10^{-4}$ atom b$^{-1}$ of $^{43}$Ca) gave better information about the wings of the resonances, especially the 1.5 keV resonance. We have reanalyzed these data by direct-

Table I. Resonance parameters from the total neutron cross section of $^{43}$Ca below 20 keV. In our notation, 1.500 2 ≡ 1.500 ± 0.002, 205 3 ≡ 205 ± 3, etc. The channel radius $a_c$ = 4.664 fm. Eigenvalues $E_\lambda$ are given in the laboratory frame.

| $E_\lambda$(keV) | $J$ | $\Gamma_{\lambda(n)}$(eV) | $\gamma^2_{\lambda(n)}$(eV) | $\gamma^2_{\lambda(n)}/E_\lambda$ | $\gamma^2_{\lambda(n)}/(E_\lambda-E_1)$ |
|---|---|---|---|---|---|
| 1.500 *2* | 4 | 205 *3* | 2610 | 1.742 | |
| 4.327 *4* | 4 | 92 *7* | 690 | 0.160 | 0.244 |
| 5.179 *8* | 3 | 85 *13* | 580 | 0.113 | 0.158 |
| 5.202 *4* | 4 | < 8 | < 50 | < 0.010 | < 0.014 |
| 6.965 *6* | 3 | 29 *11* | 170 | 0.025 | 0.031 |
| 8.860 *18* | 4 | 285 *37* | 1500 | 0.169 | 0.203 |
| 13.97 *4* | 4 | 370 *90* | 1540 | 0.111 | 0.124 |
| 19.15 *8* | 4 | 620 *180* | 2210 | 0.115 | 0.125 |

ly fitting them to Eq. (1). Corrections for Doppler and resolution broadening, being insignificant in this case, were ignored. Using the resonance parameters of Table I without modification in this analysis, the value of $\mathcal{R}_{J=4}^{\infty}$ was extracted, for later use, from the asymmetry of the resonance shape about $E_\lambda$ at the 1.5 keV resonance. This essentially single-level treatment of the earlier data gives $\mathcal{R}_{J=4}^{\text{eff}}=0.41\pm0.02$ for the very thick sample. The quantity $\mathcal{R}^{\text{eff}}$ contains the contribution to the interference asymmetry of the 1.5 keV resonance from local spin-4 levels as well as from $\mathcal{R}^{\infty}$. Consequently, the change between 1.5 keV and the thermal-neutron energy $E_{\text{th}}$ in the contribution from the known spin-4 levels must be evaluated before determining the value of $\mathcal{R}_{J=4}$ at $E_{\text{th}}$ and, hence, the scattering length $a_J$ from

$$a_J=a_c(1-\mathcal{R}_J)\ . \tag{6}$$

The value of $\mathcal{R}_{J=4}$ at $E_{\text{th}}$ also contains the major contribution resulting from the 1.5 keV resonance, which was evaluated using the parameters of Table I. We thus find $\mathcal{R}_{J=4}(E_{\text{th}})=1.85$ with about 10% uncertainty. The corresponding value of the scattering length is $a_{J=4}=-3.96$ fm with about 20% uncertainty. From this value and the value of the coherent scattering length

$$a_{\text{coh}}=\sum g_J a_J \tag{7}$$

measured as $-1.50\pm0.09$ fm [3], we find $a_{J=3}=1.66$ fm with about 50% uncertainty. The uncertainties in $a_{J=3}$ and $a_{J=4}$ are almost fully anticorrelated.

## IV. ESTIMATES OF DIRECT CAPTURE AND COMPARISON WITH DATA

The direct-capture cross section $\sigma_{\text{dir},\gamma}$ for the interaction of an $s$-wave neutron (of energy $E$) leading to a transition to a final state $f$ of spin $J_f$ can be written as [6]

$$\sigma_{\text{dir},\gamma}=\sum_J g_J\left|\sqrt{4\pi}a_c\mathcal{R}_J^{\text{loc}}\left[\frac{\Gamma_{\lambda(\gamma,\text{val})}}{\Gamma_{\lambda(n)}}\right]^{1/2}+\sigma_{\text{pot},\gamma}^{1/2}\right|^2 , \tag{8}$$

where $\mathcal{R}_J^{\text{loc}}$ is the contribution to the $\mathcal{R}$ function from local levels [see Eq. (4)], $\Gamma_{\lambda(\gamma,\text{val})}$ is the valency radiation width of the transition to the final state at $E_f$, and $\sigma_{\text{pot},\gamma}$ is the potential-capture cross section to the same state. The valence radiation width amplitude $\Gamma_{\lambda(\gamma,\text{val})}^{1/2}$ is proportional to the neutron width amplitude $\Gamma_{\lambda n}^{1/2}$ for a given spin-orbit coupling in the final state. The quantities $\Gamma_{\lambda(\gamma,\text{val})}$ and $\sigma_{\text{pot},\gamma}$ are proportional to the product of the spectroscopic factor $S$ (giving the single-particle $p$-wave admixture in the final state) and the spin-coupling factor $\mathcal{W}_{J_fj_fl_f,Jjl}$ of the squared radiative matrix element [6]. The prescriptions for calculating the valency radiative width and potential-capture cross section for a transition to a pure single-particle state in the framework of the optical model have been described in Refs. [2,5,6].

In the current work we have used, as in Refs. [2,6], the global optical-model parametrization of Moldauer [12]. For $^{43}$Ca, the potential scattering length for this optical model is 2.44 fm. The scattering length at energy $E$ for spin $J$ is

$$a_J=a_{\text{pot}}-a_c\mathcal{R}_J^{\text{loc}}\ , \tag{9}$$

and $a_c\mathcal{R}_J^{\text{loc}}$ is calculated using the spin-specific scattering lengths $a_{J=3}$ and $a_{J=4}$ discussed in Sec. III. The values of $\Gamma_{\lambda(\gamma,\text{val})}$ and $\sigma_{\text{pot},\gamma}$ are then calculated using the same optical potential. Inserting them into Eq. (8) leads to the direct-capture cross section $\sigma_{\text{dir},\gamma}$. The results are given in Table II together with the data on the final-state properties [13], especially the spectroscopic factors [9] and the experimentally known [1,8] cross sections $\sigma_{\text{exp},\gamma}$. The anticorrelated uncertainties in the scattering lengths give rise to the following uncertainties in the calculation of $\sigma_{\text{dir},\gamma}$: $\pm38\%$ ($J=2$ final state), $\pm8\%$ ($J=3$), $\mp5\%$ ($J=4$), and $\mp13\%$ ($J=5$). The compound-nuclear (CN) contribution to the cross section, deduced from the relation

$$\sigma_{\text{CN},\gamma}=(\sigma_{\text{dir},\gamma}^{1/2}\pm\sigma_{\text{exp},\gamma}^{1/2})^2\ , \tag{10}$$

is listed in the last column of Table II. In the case of a final state with an unknown spin, the $\sigma_{\text{dir},\gamma}$ and $\sigma_{\text{CN},\gamma}$ values are calculated for each possible spin. For states up to 5.4 MeV, the spin-orbit coupling $j$ is assumed to be $\frac{3}{2}$ (because the $2p_{3/2}$ orbits are filled first), but the $\frac{1}{2}$ possibility is taken into account for the higher-lying states.

The significance of the direct-capture mechanism in controlling the primary $E1$ transitions from thermal-neutron capture by $^{43}$Ca is to be assessed from the closeness of the direct-capture estimates with the experimental cross sections or, alternatively, from the smallness of the deduced compound-nuclear cross sections relative to the direct ones. Unfortunately, the spin of the corresponding final state in $^{44}$Ca is known for only 11 primary $E1$ transitions. Of these, the transitions to the seven states below 4.2 MeV show little agreement between theory and experiment (compare columns 7 and 8 of Table II), but these states have mostly small $l=1$ spectroscopic factors. The remaining four states have mostly large $l=1$ spectroscopic factors, and for these the agreement is much better. The correlation coefficient between the calculated direct-capture and experimental cross sections (both quantities divided by the gamma-ray energy) is almost 0.90.

In the 16 remaining cases (see Table II), the large difference in scattering lengths for the two initial spins causes large variation in the calculated direct-capture cross section when the assumed final-state spin value is changed. In most cases, however, it can be seen by comparing columns 7 and 8 of Table II that there is some value of the assumed spin for which the calculated cross section is similar to the experimental value. This comparison is very suggestive of the importance of the direct mechanism in this nucleus. A more quantitative analysis can be achieved by studying the reduced compound-nuclear cross sections $\sigma_{\text{CN},\gamma}/E_\gamma^3$. We first analyze these values for 14 final states below 5.4 MeV — 11 states with known spins and three with $l=1$ spectroscopic factors that are close to zero (see Table II).

The final states with spin 2 can be reached through dipole transitions only from a spin-3 initial state. The con-

Table II. Calculated direct-capture cross sections for primary $E1$ transitions from thermal-neutron capture by $^{43}$Ca compared with experimental data. Columns 1, 2, and 3 give the energy, $J^{\pi}$ value, and the $\ell = 1$ spectroscopic factor $S$ multiplied by $(2J_f + 1)$ for the final state, respectively. Column 4 is the primary transition energy. Column 5 is the average valency capture width and column 6 the potential capture cross section, both calculated using a global optical potential. The entries in column 5 do not include the spin-coupling factor and the spectroscopic factor; those in column 6 do. Column 7 is the calculated direct-capture cross section. The measured cross sections are given in column 8. Finally, column 9 gives the compound-nuclear contributions deduced via Eq. [10] from the differences between column 7 and column 8 with the +(−) sign denoting constructive(destructive) interference between the compound-nuclear and direct-capture contributions.

| Ref. [13] $E_f$ (MeV) | Ref. [13] $J_f^{\pi}$ | Ref. [9] $(d,p)$ $(2J_f+1)S^a$ | Ref. [8] $E_\gamma$ (MeV) | $\Gamma_{\gamma,\text{val}}/DE_\gamma^3$ $(10^{-7}\,\text{MeV}^{-3})$ | $\sigma_{\text{pot},\gamma}$ (mb) | $\sigma_{\text{dir},\gamma}$ (mb) | Refs. [1] and [8] $\sigma_{\text{exp},\gamma}{}^{b}$ (mb) | $\sigma_{\text{CN},\gamma}$ (mb) |
|---|---|---|---|---|---|---|---|---|
| 1.157 | $2^+$ | 0.40 | 9.974 | 0.504 | 20.3 | 26.3 | 6.8 | (−) 6.4, (+) 60 |
| 2.283 | $4^+$ | 0.064 | 8.848 | 0.592 | 10.8 | 10.8 | 22.9 | (+) 2.2, (−) 65 |
| 2.656 | $2^+$ | < 0.08 | 8.474 | 0.650 | < 4 | < 5 | 4.3 | ~ 4 |
| 3.044 | $4^+$ | strong $\ell = 3$ | 8.086 | | ~ 0 | ~ 0 | 41.5 | ~ 42 |
| 3.301 | $2^+$ | strong $\ell = 3$ | 7.829 | | ~ 0 | ~ 0 | 37.2 | ~ 37 |
| 3.357 | $(2^+ – 4^+)$ | ~ 0 | 7.773 | 0.740 | ~ 0 | ~ 0 | 188.5 | ~ 188 |
| 3.776 | 2 | ~ 0 | 7.354 | 0.770 | ~ 0 | ~ 0 | 30.4 | ~ 30 |
| 3.923 | if $3^+$ | 0.32 | 7.208 | 0.782 | 11.6 | 26.1 | 96.1 | (+) 22, (−) 222 |
| | if $4^+$ | | | | | 41.3 | | (+) 11, (−) 263 |
| | if $5^+$ | | | | | 60.3 | | (+) 4, (−) 309 |
| 4.196 | $2^+$ | 0.16 | 6.935 | 0.824 | 5.6 | 7.0 | 54.6 | (+) 23, (−) 101 |
| 4.480 | $2^+$ | 0.32 | 6.651 | 0.872 | 10.7 | 13.4 | 26.0 | (+) 2, (−) 77 |
| 4.584 | $(2^+ – 4^+)$ | ~ 0 | 6.547 | 0.887 | ~ 0 | ~ 0 | 146.3 | ~ 146 |
| 4.651 | $2^+$ | 2.24 | 6.480 | 0.904 | 72.7 | 91.1 | 142.6 | (+) 6, (−) 461 |
| 4.690 | $(1^- – 4^+)$ | ~ 0 | 6.441 | 0.910 | ~ 0 | ~ 0 | 24.2 | ~ 24 |
| 4.914 | if $2^+$ | 0.96 | (6.217) | 0.955 | 29.8 | 36.3 | ~ 0 | ~ 36 |
| | if $3^+$ | | | | | 64.7 | | ~ 65 |
| | if $4^+$ | | | | | 101.4 | | ~ 101 |
| | if $5^+$ | | | | | 147.2 | | ~ 147 |
| 4.992 | if $2^+$ | 0.40 | (6.139) | 0.972 | 12.3 | 14.9 | ~ 0 | ~ 15 |
| | if $3^+$ | | | | | 26.5 | | ~ 27 |
| | if $4^+$ | | | | | 41.5 | | ~ 42 |
| | if $5^+$ | | | | | 60.3 | | ~ 60 |
| 5.006 | $4^+$ | 2.00 | 6.125 | 0.975 | 61.0 | 207 | 230.6 | (+) 1, (−) 875 |
| 5.130 | if $2^+$ | 0.96 | 6.001 | 1.002 | 28.7 | 34.8 | 210.2 | (+) 74, (−) 416 |
| | if $3^+$ | | | | | 61.9 | | (+) 44, (−) 500 |
| 5.231 | if $2^+$ | 4.32 | 5.901 | 1.024 | 126.8 | 153.7 | 432 | (+) 70, (−) 1100 |
| | if $3^+$ | | | | | 273.2 | | (+) 18, (−) 1390 |
| | if $4^+$ | | | | | 425.0 | | (+) 0.03, (−) 1710 |
| | if $5^+$ | | | | | 615.8 | | (−) 16, (−) 2080 |
| 5.289 | if $2^+$ | 2.16 | 5.842 | 1.039 | 63.4 | 76.0 | 72.5 | (−) 0.04, (−) 297 |
| | if $3^+$ | | | | | 134.5 | | (−) 10, (−) 404 |
| | if $4^+$ | | | | | 209.6 | | (−) 36, (−) 529 |
| | if $5^+$ | | | | | 303.6 | | (−) 79, (−) 673 |
| 5.342 | $2^+$ | 2.24 | 5.789 | 1.050 | 64.4 | 78.0 | 21.7 | (−) 17, (−) 182 |

Table II. *(Continued)*.

| Ref. [13] $E_f$ (MeV) | Ref. [13] $J_f^\pi$ | Ref. [9] $(d,p)$ $(2J_f+1)S$ [a] | Ref. [8] $E_\gamma$ (MeV) | $\Gamma_{\gamma,\mathrm{val}}/DE_\gamma^3$ $(10^{-7}\mathrm{MeV}^{-3})$ | $\sigma_{\mathrm{pot},\gamma}$ (mb) | Refs. [1] and [8] $\sigma_{\mathrm{dir},\gamma}$ (mb) | $\sigma_{\mathrm{exp},\gamma}$ [b] (mb) | $\sigma_{\mathrm{CN},\gamma}$ (mb) |
|---|---|---|---|---|---|---|---|---|
| 5.375[a] | if $2^+$ | 0.56 | 5.756 | 1.059 | 16.0 | 19.4 | 52.7 | (+) 8, (–) 136 |
| | if $3^+$ | | | | | 34.2 | | (+) 2, (–) 172 |
| | if $4^+$ | | | | | 53.2 | | (–) 0.001, (–) 212 |
| | if $5^+$ | | | | | 77.1 | | (–) 2, (–) 257 |
| 5.459 | if $2^+$ | 2.64 | 5.673 | 1.079 | 74.2 | 89.8 | 31.0 | (–) 15, (–) 226 |
| | if $3^+$ $(j=\frac{3}{2})$ | | | | | 158.2 | | (–) 49, (–) 329 |
| | if $3^+$ $(j=\frac{1}{2})$ | | | | | 229.0 | | (–) 91, (–) 429 |
| | if $4^+$ $(j=\frac{3}{2})$ | | | | | 246.1 | | (–) 102, (–) 452 |
| | if $4^+$ $(j=\frac{1}{2})$ | | | | | 159.3 | | (–) 50, (–) 331 |
| 5.549 | if $2^+$ | 3.20 | 5.582 | 1.102 | 88.4 | 106.9 | 61.4 | (–) 6, (–) 330 |
| | if $3^+$ $(j=\frac{3}{2})$ | | | | | 187.8 | | (–) 34, (–) 464 |
| | if $3^+$ $(j=\frac{1}{2})$ | | | | | 271.2 | | (–) 75, (–) 591 |
| | if $4^+$ $(j=\frac{3}{2})$ | | | | | 291.8 | | (–) 85, (–) 621 |
| | if $4^+$ $(j=\frac{1}{2})$ | | | | | 189.3 | | (–) 35, (–) 466 |
| 5.733 | if $2^+$ | 6.00 | 5.398 | 1.152 | 159.8 | 192.7 | 232.5 | (+) 2, (–) 849 |
| | if $3^+$ $(j=\frac{3}{2})$ | | | | | 337.1 | | (–) 10, (–) 1130 |
| | if $3^+$ $(j=\frac{1}{2})$ | | | | | 488.2 | | (–) 47, (–) 1395 |
| | if $4^+$ $(j=\frac{3}{2})$ | | | | | 522.4 | | (–) 58, (–) 1450 |
| | if $4^+$ $(j=\frac{1}{2})$ | | | | | 340.4 | | (–) 10, (–) 1136 |
| | if $5^+$ | | | | | 754.3 | | (–) 149, (–) 1824 |
| 5.867 | if $2^+$ | 1.28 | 5.264 | 1.191 | 33.1 | 39.9 | 73.8 | (+) 5, (–) 222 |
| | if $3^+$ $(j=\frac{3}{2})$ | | | | | 69.4 | | (+) 0.1, (–) 286 |
| | if $3^+$ $(j=\frac{1}{2})$ | | | | | 100.7 | | (–) 2, (–) 347 |
| | if $4^+$ $(j=\frac{3}{2})$ | | | | | 107.5 | | (–) 3, (–) 359 |
| | if $4^+$ $(j=\frac{1}{2})$ | | | | | 70.4 | | (+) 0.04, (–) 288 |
| | if $5^+$ | | | | | 155.3 | | (–) 15, (–) 443 |
| 6.040 | if $2^+$ | 0.64 | 5.092 | 1.243 | 16.0 | 19.2 | 24.8 | (+) 0.4, (–) 88 |
| | if $3^+$ $(j=\frac{3}{2})$ | | | | | 33.3 | | (–) 0.6, (–) 116 |
| | if $3^+$ $(j=\frac{1}{2})$ | | | | | 48.3 | | (–) 4, (–) 142 |
| | if $4^+$ $(j=\frac{3}{2})$ | | | | | 51.4 | | (–) 5, (–) 148 |
| | if $4^+$ $(j=\frac{1}{2})$ | | | | | 33.7 | | (–) 0.7, (–) 116 |
| | if $5^+$ | | | | | 74.0 | | (–) 13, (–) 184 |
| 6.146 | if $2^+$ | 3.68 | 4.984 | 1.278 | 89.7 | 107.7 | 69.4 | (–) 4, (–) 350 |
| | if $3^+$ $(j=\frac{3}{2})$ | | | | | 186.2 | | (–) 28, (–) 483 |
| | if $3^+$ $(j=\frac{1}{2})$ | | | | | 269.7 | | (–) 66, (–) 613 |
| | if $4^+$ $(j=\frac{3}{2})$ | | | | | 286.9 | | (–) 74, (–) 639 |
| | if $4^+$ $(j=\frac{1}{2})$ | | | | | 188.8 | | (–) 29, (–) 487 |
| | if $5^+$ | | | | | 412.9 | | (–) 144, (–) 821 |

[a] For states below this energy, the spin-orbit coupling $j$ was assumed to be $\frac{3}{2}$.

[b] Uncertain by 5-10% and 10%, respectively, due to the uncertainties in the measured branching ratios (Ref. [8]) and total capture cross section (Ref. [1]).

tribution to the compound-nuclear capture from the known spin-3 resonances (see Table I) is only ~3% of that from the 1.5 keV resonance. Therefore, the compound-nuclear cross sections for these transitions should be smaller than those to final states with spins 3–5, which we expect will be controlled predominantly by the spin-4 resonance at 1.5 keV. From general considerations of the spin dependence of the level density, we would not expect to find many more than the eight spin-2 final states out of the 27 entries in Table II. Hence, we assumed that all states in that table with uncertain spins have $J>2$.

The average compound-nuclear contribution from the spin-3 resonances can be estimated as $\langle \sigma_{\mathrm{CN},\gamma}/E_\gamma^3 \rangle = 0.044\ \mathrm{mb\,MeV}^{-3}$ by limiting the averaging to the known spin-2 states and by using the smaller value when two are listed in the last column of Table II. For the remaining states with known spin or unique $\langle \sigma_{\mathrm{CN},\gamma}/E_\gamma^3 \rangle$ value (the latter because either $\sigma_{\mathrm{dir},\gamma}$ or $\sigma_{\mathrm{exp},\gamma}$ is zero), we obtain $\langle \sigma_{\mathrm{CN},\gamma}/E_\gamma^3 \rangle = 0.18\ \mathrm{mb\,MeV}^{-3}$. Subtracting from this value the expected contribution from the spin-3 resonances (about 0.04 mb $\mathrm{MeV}^{-3}$), we find 0.14 mb $\mathrm{MeV}^{-3}$ as the average compound-nuclear contribution from the 1.5 keV, spin-4 resonance. The individual fluctuations about this value are large, but by using maximum likelihood analysis, we find that they are, as expected, consistent with a Porter-Thomas distribution. We can also compare this mean with the value of $\sigma_{\mathrm{CN},\gamma}/E_\gamma^3$ to be expected from Cameron's [14] semiempirical model (see Eqs. (9)–(12) of Ref. [2]). The model value (for an assumed spin-4 resonance spacing of 3.5 keV) is 0.08 $\mathrm{mb\,MeV}^{-3}$; this value is in reasonable agreement with 0.14 $\mathrm{mb\,MeV}^{-3}$ deduced above. The average reduced cross section from the spin-3 resonances is one-third of that from the spin-4 1.5 keV resonance rather than the 3% suggested by the known resonance parameters. This observation together with the value of the spin-3 scattering length suggests a weak and weakly bound $3^-$ level as the main contributor to the spin-3 component of the cross section.

With these estimates for the compound-nuclear cross sections, we can assign possible spin values for the remaining final states if we add the criterion that the individual $\sigma_{\mathrm{CN},\gamma}/E_\gamma^3$ value should be less than about four times the mean (thus encompassing about 96% of the transitions in a Porter-Thomas distribution). We find that for all transitions there is at least one spin value (for the final state) that gives a calculated direct-capture cross section that is qualitatively consistent with the experiment. Furthermore, the possible distribution of final-state spins is reasonably balanced, and so is the possible pattern of destructive or constructive interference between the direct and compound-nuclear amplitudes.

## V. DISCUSSION

In Sec. IV, we have presented a consistent physical picture of thermal-neutron capture by $^{43}$Ca. Direct capture is the most important mechanism for the majority of states up to an excitation energy of 6.2 MeV (which is as high as we can go on the basis of known spectroscopic factors). To obtain the total direct-capture cross section for these states, we first select the most likely $J>2$ spin value for states with unknown spins on the basis of small compound-nuclear cross section (that is, consistent with the Cameron relation), sum the direct-capture estimates appropriate to these spin choices, then do the same for states with known spins, and add the two summed values. We find

$$\sigma_{\mathrm{dir},\gamma}(E_f < 6.2\ \mathrm{MeV}) = 2.08\ \mathrm{b}\ .$$

For the same spin selections, the summed compound-nuclear capture is

$$\sigma_{\mathrm{CN},\gamma}(E_f < 6.2\ \mathrm{MeV}) = 0.84\ \mathrm{b}\ .$$

The sum of the experimental values of the cross sections is

$$\sigma_{\mathrm{exp},\gamma}(E_f < 6.2\ \mathrm{MeV}) = 2.33\ \mathrm{b}\ .$$

The difference between this value and the sum of the direct and compound-nuclear estimates can quite reasonably be attributed to the statistical fluctuations of the interference terms.

We may also make estimates of the compound-nuclear capture cross sections for all positive-parity states up to 6.2 MeV using Cameron's model and the parameters of the 1.5 keV resonance. The total is

$$\sigma_{\mathrm{Cameron},\gamma}(E_f < 6.2\ \mathrm{MeV}) = 0.5\ \mathrm{b}\ ,$$

again consistent with 0.84 b deduced previously.

For the states above 6.2 MeV, we can make a statistical-model estimate of the compound-nuclear contribution starting with an estimate of the level-density function for $^{44}$Ca. From the known level scheme [13], we have a reliable estimate of the density of levels with spins ranging from 2 to 5 in the region of 5 MeV excitation energy, and from the neutron resonances [1] we know the density of spin-3 and spin-4 levels at the neutron separation energy of 11.13 MeV. We assume that there is no significant dependence on parity and write the functional dependence of the level density on excitation energy and spin as

$$\rho(E,J) = \rho_0(2J+1)\exp[-(J+\tfrac{1}{2})^2/2\sigma^2]\exp(E/T)\ . \tag{11}$$

The value of the spin dispersion coefficient $\sigma$ is taken from a study by Newton [15] of the effect of the shell model on the Fermi gas level-density parameters. The data are consistent with $\rho_0 = 0.043\ \mathrm{MeV}^{-1}$ and $T = 1.48$ MeV. Newton's $\sigma^2 = 7$ value is consistent with the distribution of the preferred spin values of final states used in the direct-capture analysis. With this statistical representation for levels above 6.2 MeV, we obtain a total radiation width for neutron capture to these states of 0.18 eV, and this width gives rise to a compound-nuclear contribution of 0.9 b. We assume an additional contribution from the hypothesized weakly bound $3^-$ level of about one-third of this value. Added to the previously deduced CN cross section to the states below 6.2 MeV, the total CN capture cross section is 1.7 b. After allowing for the calculated direct-capture cross section of 2.08 b, there is still a shortfall of 2.4 b against the experimentally measured total capture cross section of $6.2\pm0.6$ b.

This shortfall is in the medium- and low-energy group of primary transitions (below 5 MeV). While the total strength of the single-particle $2p$ state is not exhausted by the final states below 6.2 MeV (the spectroscopic factors account for about 80% of the theoretical maximum), the remainder will allow only about 0.6 b of additional direct capture. It thus appears that the Cameron model [14], while being approximately consistent with the high-energy primary transitions, gives too low an estimate for the lower-energy group by about a factor of 2. The other models developed for neutron-resonance capture by Brink [16] and by Kadmenskij, Markushev, and Furman [17] fail even more badly in redressing this overall balance in spectral shape, both of them accentuating the high-energy transitions by virtue of the central role played by the giant electric-dipole resonance. Magnetic-dipole transitions could be playing some role in the missing cross section; however, few of these have been identified (accounting for $\sim 0.3$ b) in the resolved spectrum [8].

Some data are available on the total radiation widths of the higher-energy neutron resonances in $^{43}$Ca [7]; the average radiation width of the spin-4 resonances is $650\pm40$ meV. This value can also be compared with the Cameron semiempirical relation [14] (with $E_\gamma$ in MeV)

$$\Gamma_\gamma/D = 0.33\times10^{-9}E_\gamma^3 A^{2/3} , \quad (12)$$

which gives a total radiation width of 290 meV. The total valence radiation width is estimated to be

$$36\Gamma(\mathrm{eV})/\sqrt{E(\mathrm{eV})}\ \mathrm{meV} .$$

If the valence components are subtracted from the resonance radiation widths, the average of residues (estimated compound-nuclear radiation widths) is 560 meV, again demonstrating that the Cameron model value is low by about a factor of 2. The total valence radiation width of the 1.5 keV resonance is 190 meV, which, on its own, would account for 1 b of the thermal-neutron capture cross section. Our estimate of the direct-capture cross section is 2.08 b. The difference results from constructive interference between the valence capture from the wings of nearby resonances and potential capture related to the potential scattering length. This interference effect also accounts for the fact that the thermal-neutron capture spectrum [8] is not quantitatively similar to that inferred in Ref. [7] from resonance capture.

## VI. SUMMARY

We have identified $^{43}$Ca as a nucleus in which the thermal-neutron capture shows a strong interplay between direct and compound-nuclear mechanisms. We have determined the neutron widths of the ($s$-wave) resonances in this region and deduced their total angular momenta. From these data and the previously measured coherent scattering length of this rare isotope, we have made fairly accurate estimates of the scattering lengths for the two $s$-wave spin states at thermal-neutron energy. This information has enabled us to make a detailed analysis of the mechanisms controlling the thermal-neutron capture gamma-ray spectrum.

While the evidence for the direct process is not as overwhelming (because of the strong influence of the resonance at 1.5 keV) as it is for most of the even isotopes of calcium, it is nevertheless very persuasive. For several of the final states with known spins and large spectroscopic factors, a strong correlation exists between the calculated direct-capture and experimental cross sections. For the positive-parity states below 6.2 MeV with known spectroscopic factors, the estimated total direct-capture cross section amounts to 90% of the total experimental value. An analysis of the possible compound-nuclear contribution to these states, after removing the direct-capture component, is consistent with a reasonable spin distribution for the final states and with the Cameron estimate of the compound-nuclear cross section.

More than 50% of the total capture cross section has been attributed [8] to unresolved primary transitions to final states above 6.2 MeV. Direct capture can account for only a small portion of their total intensity ($\sim 0.6$ b out of $\sim 3.3$ b). The available compound-nuclear capture models for electric-dipole transitions cannot adequately explain the difference, and it is not known whether there is a substantial magnetic-dipole contribution at these lower gamma-ray energies. Details of the gamma-ray spectrum, particularly to states above 6.2 MeV, are desirable with a view to elucidating the nature of the compound-nuclear process.

## ACKNOWLEDGMENTS

One of us (M.C.M) is grateful to the Oak Ridge National Laboratory for its hospitality. The research described in this paper was sponsored by the U.S. Department of Energy under Contract Nos. DE-AC05-84OR21400 with Martin Marietta Energy Systems, Inc. (Oak Ridge) and W-7405-eng-36 with the University of California (Los Alamos).

[1] S. F. Mughabghab, M. Divadeenam, and N. E. Holden, *Neutron Cross Sections,* Vol. 1, Part A (Academic, New York, 1981).
[2] S. Kahane, J. E. Lynn, and S. Raman, Phys. Rev. C **36**, 533 (1987).
[3] S. Raman, S. Kahane, R. M. Moon, J. A. Fernandez-Baca, J. L. Zarestky, J. E. Lynn, and J. W. Richardson, Phys. Rev. C **39**, 1297 (1989).
[4] S. Raman, J. A. Fernandez-Baca, R. M. Moon, and J. E. Lynn, Phys. Rev. C **44**, 518 (1991).
[5] A. M. Lane and J. E. Lynn, Nucl. Phys. **17**, 563 (1960); **17**, 586 (1960).
[6] S. Raman, R. F. Carlton, J. C. Wells, E. T. Jurney, and J. E. Lynn, Phys. Rev. C **32**, 18 (1985).
[7] A. R. de L. Musgrove, B. J. Allen, J. W. Boldeman, D. M. H. Chan, and R. L. Macklin, Nucl. Phys. **A279**, 317 (1977).
[8] D. H. White and R. E. Birkett, Phys. Rev. C **5**, 513 (1972).

See also W. Ratynski, P. H. M. Van Assche, H. Börner, W. F. Davidson, and J. A. Pinston, in *Proceedings of the International Conference on the Interactions of Neutrons with Nuclei,* Lowell, Massachusetts, 1976, edited by E. Sheldon (Energy Research and Development Administration Report CONF-7560715-P2, 1976), p. 1301.

[9] J. H. Bjerregaard and O. Hansen, Phys. Rev. **155**, 1229 (1967).

[10] J. E. Lynn and S. Raman, in *Capture Gamma-Ray Spectroscopy,* Proceedings of the Seventh International Symposium on Capture Gamma Ray Spectroscopy and Related Topics, edited by R. W. Hoff, AIP Conf. Proc. No. 238 (AIP, New York, 1991), p. 555.

[11] M. C. Moxon, "A Least-Squares Fitting for Resonance Analysis of Neutron Transmission and Capture Data," Harwell (UK) AEA Technology Report No. AEA-INTEC-0470, 1991 (unpublished).

[12] P. A. Moldauer, Nucl. Phys. **47**, 65 (1963).

[13] P. M. Endt, Nucl. Phys. **A521**, 1 (1990).

[14] A. G. W. Cameron, Can. J. Phys. **37**, 322 (1959).

[15] T. D. Newton, Can. J. Phys. **34**, 804 (1956).

[16] D. M. Brink, Ph.D. thesis, Oxford University, 1955 (unpublished).

[17] S. G. Kadmenskij, V. P. Markushev, and V. I. Furman, Yad. Fiz. **37**, 277 (1983) [Sov. J. Nucl. Phys. **37**, 165 (1983)].